Supporting Information

Ortho- Hydroxylation of Aromatic Acids by a non-heme Fe^{V}=O species: How important is the ligand design?

Azaj Ansari and Gopalan Rajaraman*

Department of Chemistry, Indian Institute of Technology Bombay, Mumbai-400076, India

Email: rajaraman@chem.iitb.ac.in

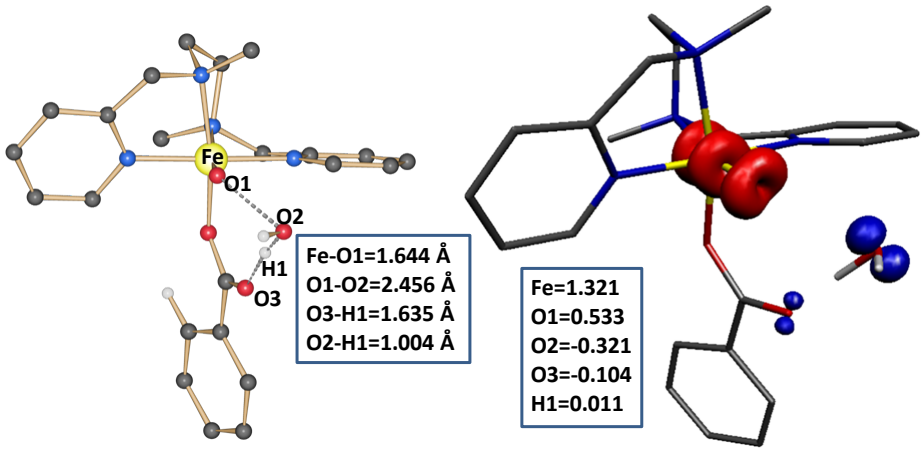

(a) (b)

Figure S1. B3LYP computed a) optimized structure and b) spin density plot of the ground state (^{2}II-*ts1*).

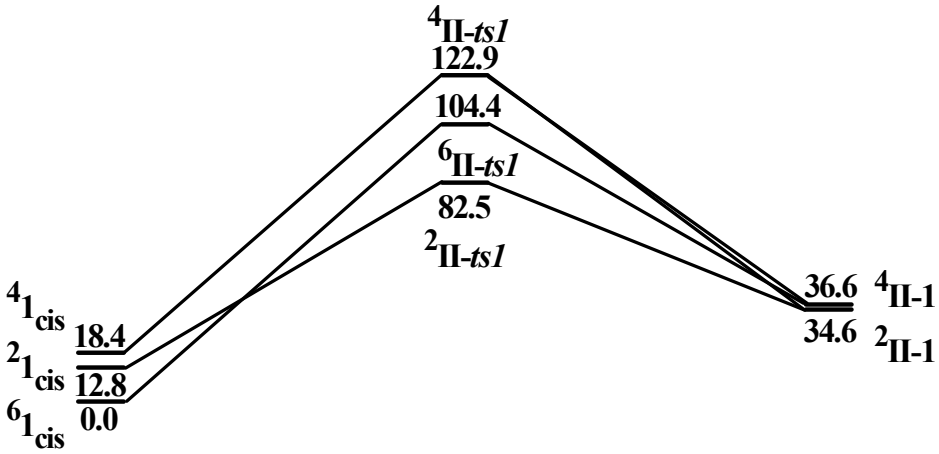

Figure S2. B3LYP computed potential energy surface (ΔG in kJ/mol) for the O…O cleavage starting from 1_{cis} species.

Table S1. Computed bond parameters (in *Angstroms) of transition states and* Fe^{V}*=O species.*

B3LYP-D Functional						
II-*ts1*	Fe-O1	O1-O2	O3-H1	O2-H1		
^{6}II-*ts1*	1.684	1.968	1.018	1.612		
^{4}II-*ts1*	1.721	1.780	1.023	1.576		
^{2}II-*ts1*	1.651	2.450	1.534	1.019		
II-**1**	Fe-O1	Exp[1]				
^{4}II-**1**	1.652	1.58				
^{2}II-**1**	1.654					
III-*ts1*	Fe-O1	O1-O2				
^{6}III-*ts1*	1.672	2.015				
II-1	Fe-O1	Fe-O2	Fe-N1	Fe-N2	Fe-N3	Fe-N4
^{2}II-1(BPMEN)	1.654	1.988	1.989	2.129	2.035	2.000
^{2}II-1(TPA)[2]	1.651	1.993	1.971	2.109	1.965	1.974
II-*ts1*						
^{2}II-*ts1*(BPMEN)	1.656	1.935	1.978	2.130	2.045	2.011
^{2}II-*ts1*(TPA)[2]	1.654	1.932	1.980	2.088	1.972	1.968

B3LYP Functional						
II-*ts1*	Fe-O1	O1-O2	O3-H1	O2-H1		
^{6}II-*ts1*	1.684	1.968	1.018	1.612		
^{4}II-*ts1*	1.721	1.800	1.023	1.576		
^{2}II-*ts1*	1.644	2.456	1.635	1.004		
II-**1**	Fe-O1	Exp[1]				
^{4}II-**1**	1.657	1.58				
^{2}II-**1**	1.651					
III-*ts1*	Fe-O1	O1-O2				
^{6}III-*ts1*	1.669	2.048				
^{4}III-*ts1*	1.654	2.928				
^{2}III-*ts1*	1.656	2.594				
II-*ts1*	Fe-O1	Fe-O2	Fe-N1	Fe-N2	Fe-N3	Fe-N4
^{2}II-*ts1*(BPMEN)	1.658	1.923	1.991	2.151	2.069	2.016
^{2}II-*ts1*(TPA)[2]	1.708	1.863	1.980	2.054	1.995	1.989

Table S2. B3LYP-D computed spin expectation values of Iron species.

BPMEN	<S**2>	Expected Spin	<S**2>	Expected Spin
	BPMEN		TPA	
1_{cis}				
$^{6}1_{cis}$	8.7601	8.75	8.7593	8.75
$^{4}1_{cis}$	3.8076	3.75	3.8020	3.75
$^{2}1_{cis}$	0.7825	0.75	0.7864	0.75
II-*ts1*				
^{6}II-*ts1*	8.8563	8.75	8.8486	8.75
^{4}II-*ts1*	3.8406	3.75		-
^{2}II-*ts1*	1.6603	0.75	1.4994	0.75
1_{trans}				
$^{6}1_{trans}$	8.7616	8.75	8.7616	8.75
$^{4}1_{trans}$	3.8062	3.75	3.8051	3.75
$^{2}1_{trans}$	0.7744	0.75	0.7754	0.75
III-*ts1*				
^{6}III-*ts1*	8.8477	8.75	8.8486	8.75
^{4}III-*ts1*	3.7719	3.75	3.8239	3.75
^{2}III-*ts1*	1.7343	0.75	1.6382	0.75
III-**1**				
^{5}III-**1**	6.0608	6.00	6.0558	6.00
^{3}III-**1**	2.0227	2.00	2.0191	2.00
^{1}III-**1**	0.0000	0.00	0.0000	0.00
II-**1**				
^{4}II-**1**	4.7814	3.75	3.7814	3.75
^{2}II-**1**	1.7770	0.75	1.7746	0.75
II-*ts2*				
^{4}II-*ts2*	4.6105	3.75	3.8039	3.75
^{2}II-*ts2*	1.6724	0.75	1.6452	0.75
II-**2**				
^{6}II-**2**	8.7604	8.75	8.7607	8.75
^{4}II-$\mathbf{2}_{is}$	3.8129	3.75	3.8004	3.75
^{2}II-$\mathbf{2}_{ls}$	0.7824	0.75	0.7807	0.75
II-*ts3*				
^{6}II-*ts3*	8.7599	8.75	8.7609	8.75
^{4}II-*ts3*	3.8083	3.75	3.7992	3.75
^{2}II-*ts3*	0.7861	0.75	0.7757	0.75
II-**3**				
^{6}II-**3**	8.7595	8.75	8.7610	8.75
^{4}II-**3**	3.8133	3.75	3.7911	3.75
^{2}II-**3**	0.7841	0.75	0.7722	0.75

1				
^{6}**1**	8.7588	8.75	8.7621	8.75
^{4}**1**	3.8245	3.75	3.8169	3.75
^{2}**1**	0.8629	0.75	1.0546	0.75
II-**1**				
^{4} II(1)-**1A**	4.7814	3.75		
^{2} II(1)-**1A**	1.7770	0.75		
^{4} II(1)-**1B**	4.8140	3.75		
^{2} II(1)-**1B**	1.7853	0.75		
^{4} II(1)-**1C**	4.8254	3.75		
^{2} II(1)-**1C**	1.7876	0.75		

Table S3. B3LYP-D computed Mulliken charge of Iron species.

$[(BPMEN)Fe^{III}\text{-}OOH]^{2+}$ species			
	Fe	O1	O2
1_{cis}			
$^{6}1_{cis}$	2.005	-0.322	-0.523
$^{4}1_{cis}$	1.671	-0.242	-0.529
$^{2}1_{cis}$	1.378	-0.241	-0.547
II-*ts1*			
^{6}II-*ts1*	1.748	-0.065	-0.517
^{4}II-*ts1*	1.398	0.1847	-0.729
^{2}II-*ts1*	0.611	-0.324	0.230
1_{trans}			
$^{6}1_{trans}$	1.790	-0.166	-0.450
$^{4}1_{trans}$	1.582	-0.243	-0.433
$^{2}1_{trans}$	1.283	-0.228	-0.427
III-*ts1*			
^{6}III-*ts1*	1.607	-0.113	-0.423
^{4}III-*ts1*	1.538	-0.388	-0.225
^{2}III-*ts1*	1.375	-0.470	-0.264

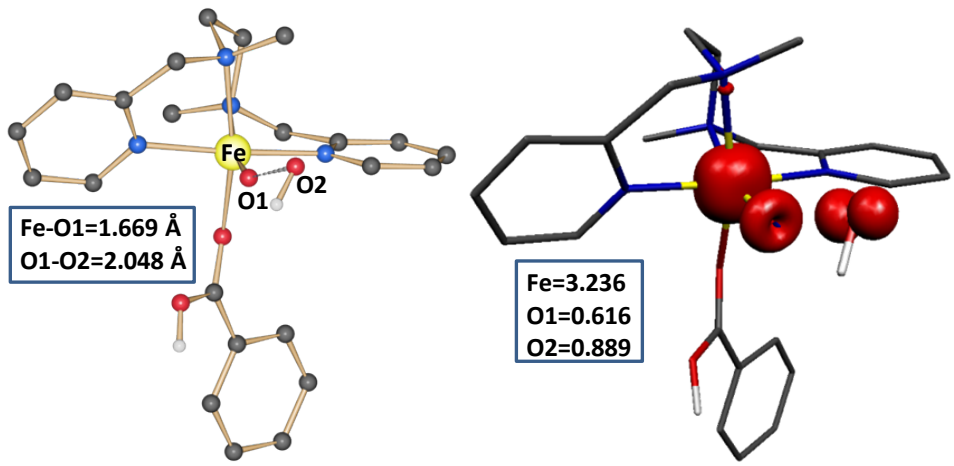

Figure S3. B3LYP computed a) optimized structure and b) spin density plot of the ground state (^{6}III-*ts1*).

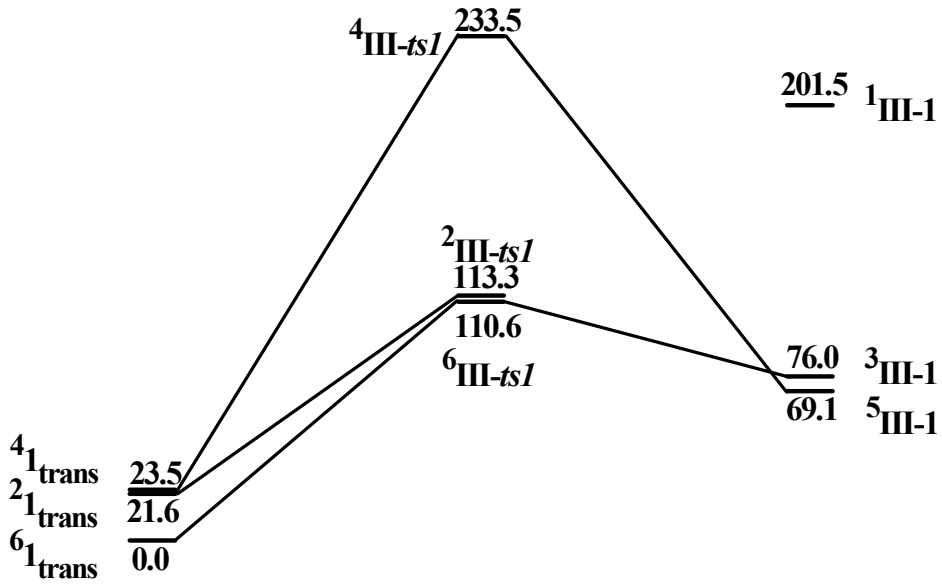

Figure S4. B3LYP computed potential energy surface (ΔG in kJ/mol) for the O...O bond cleavage starting from $\mathbf{1}_{trans}$ species.

Note:- Although all the structures were successfully optimized with B3LYP-D functionals, transition states ^{4}III-*ts1 and* ^{2}III-*ts1* could not be achieved. For these two species single point B3LYP-D calculations on the B3LYP geometries are performed. As these transition states are high-lying, these are unlikely to affect the mechanistic conclusions derived.

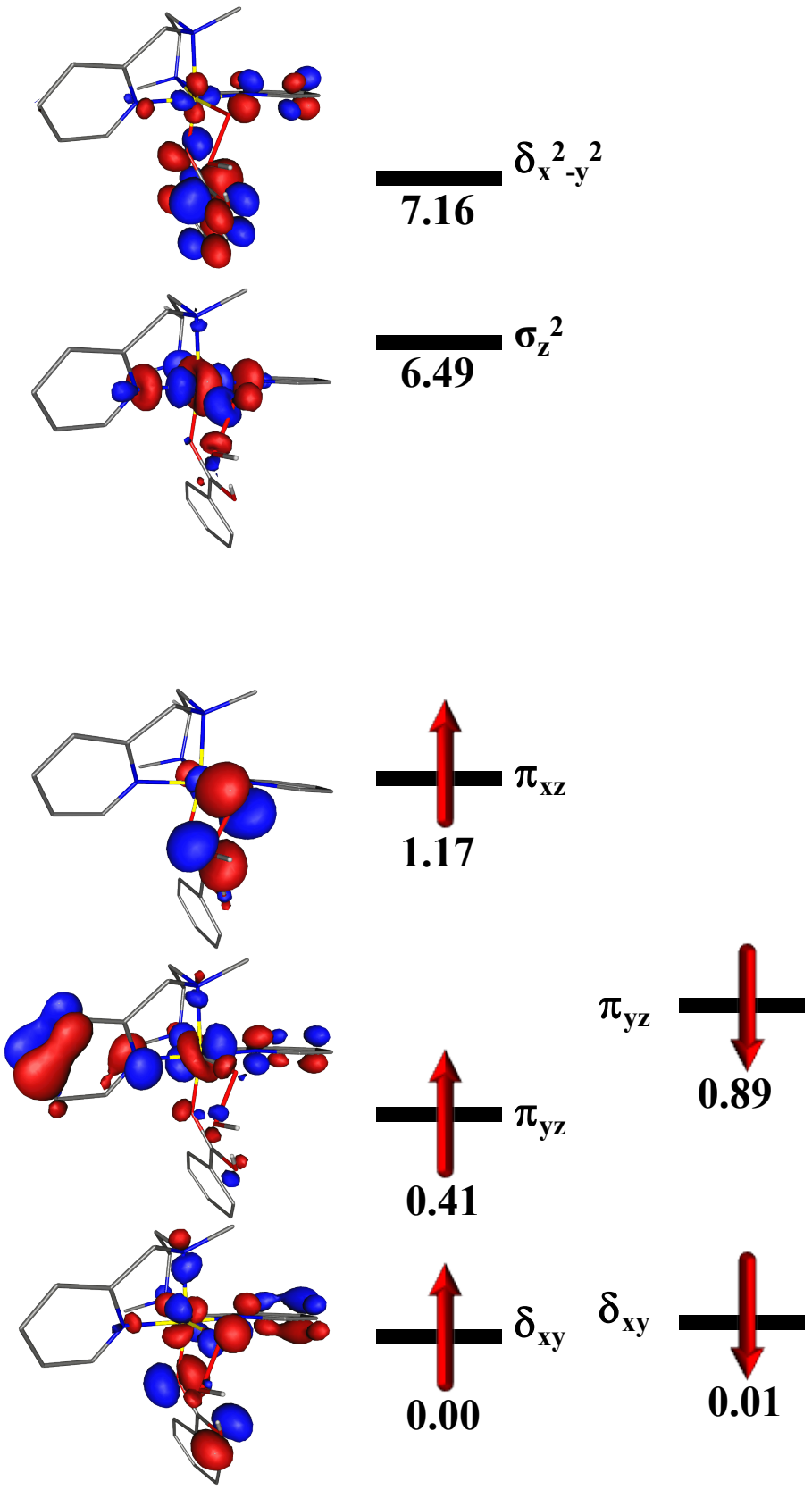

Figure S5. B3LYP-D computed Eigen-value plot incorporating energies computed for d-based orbitals for $^{2}1_{cis}$ species (energies are given in eV).

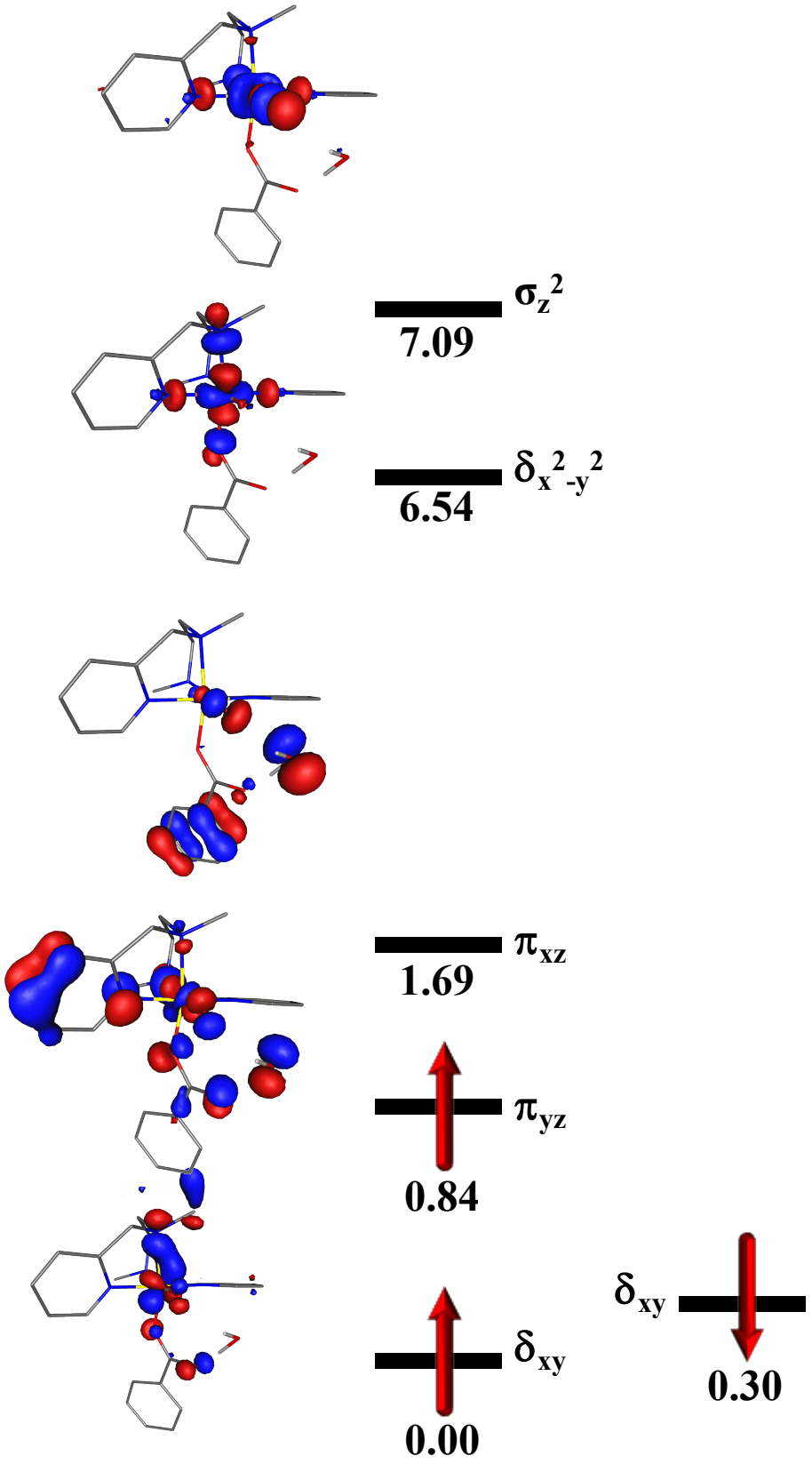

Figure S6. B3LYP-D computed Eigen-value plot incorporating energies computed for d-based orbitals for ^{2}II-*ts1* species (energies are given in eV).

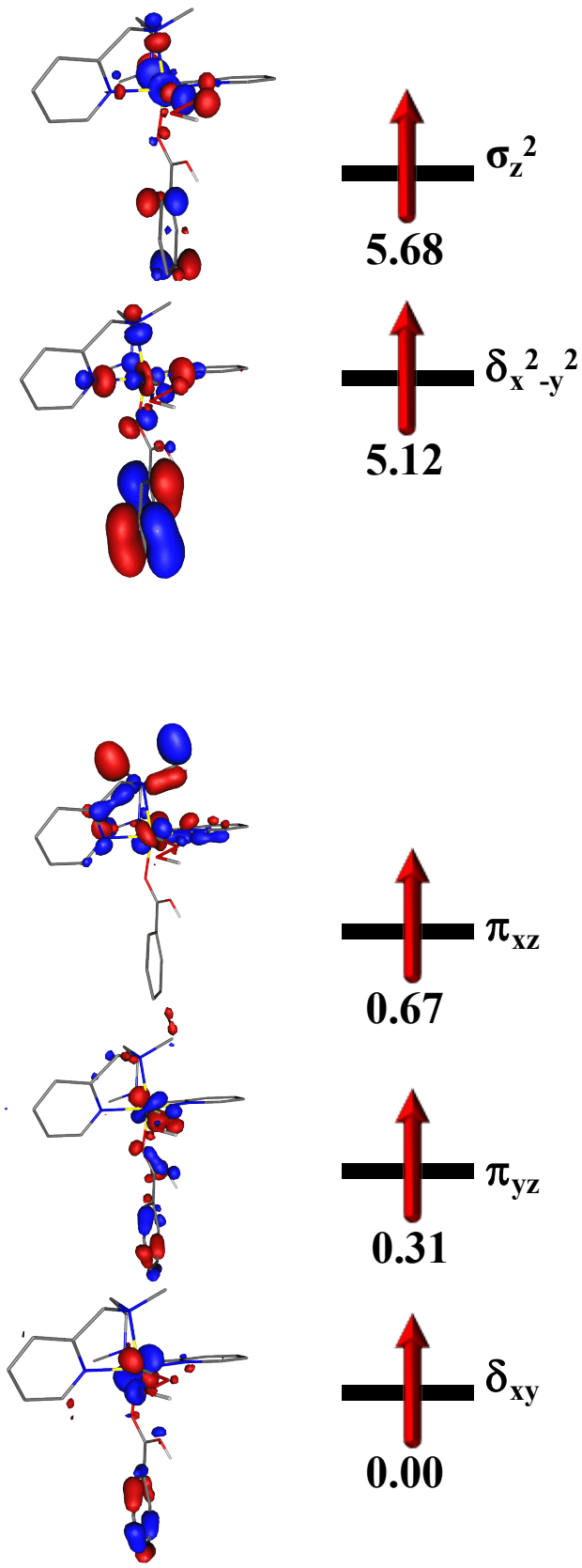

Figure S7. B3LYP-D computed Eigen-value plot incorporating energies computed for d-based orbitals for $^{6}1_{trans}$ species (energies are given in eV).

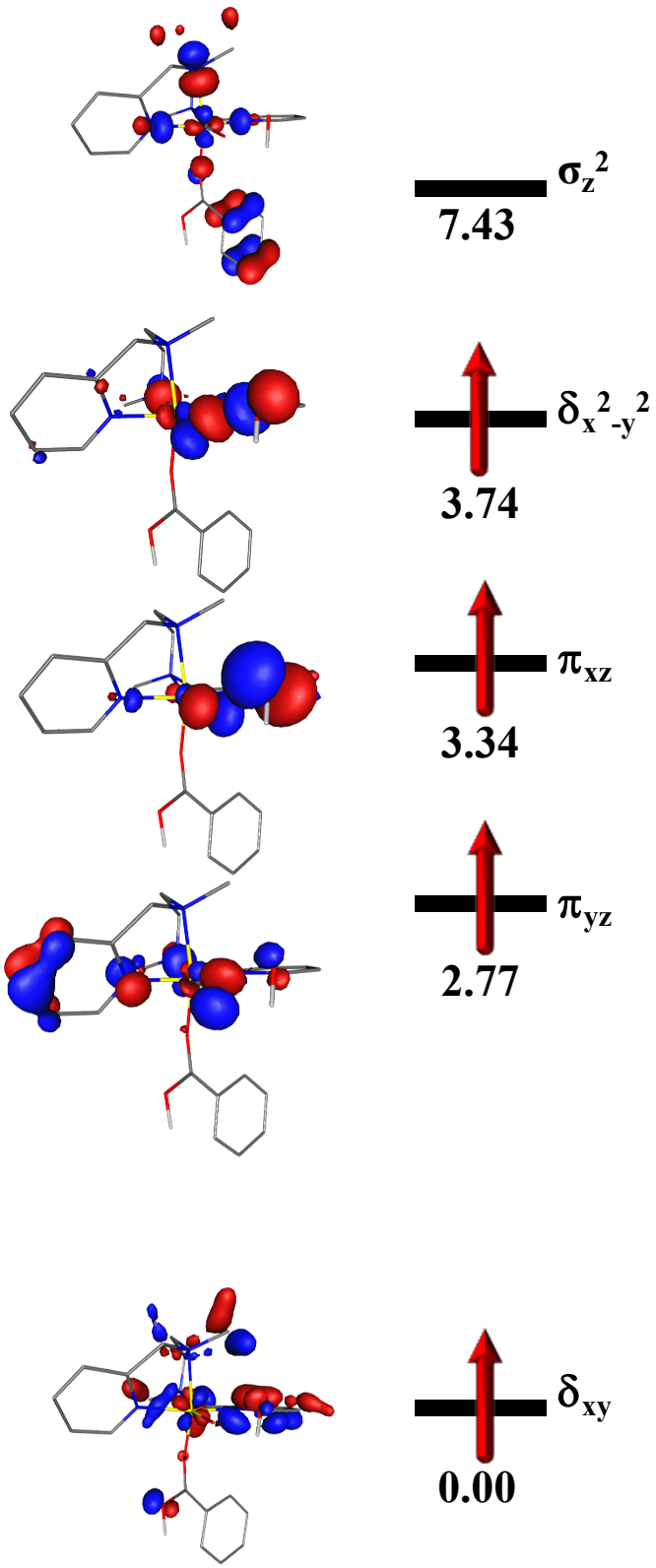

Figure S8. B3LYP-D computed Eigen-value plot incorporating energies computed for d-based orbitals for ^{6}III-*ts1* species (energies are given in eV).

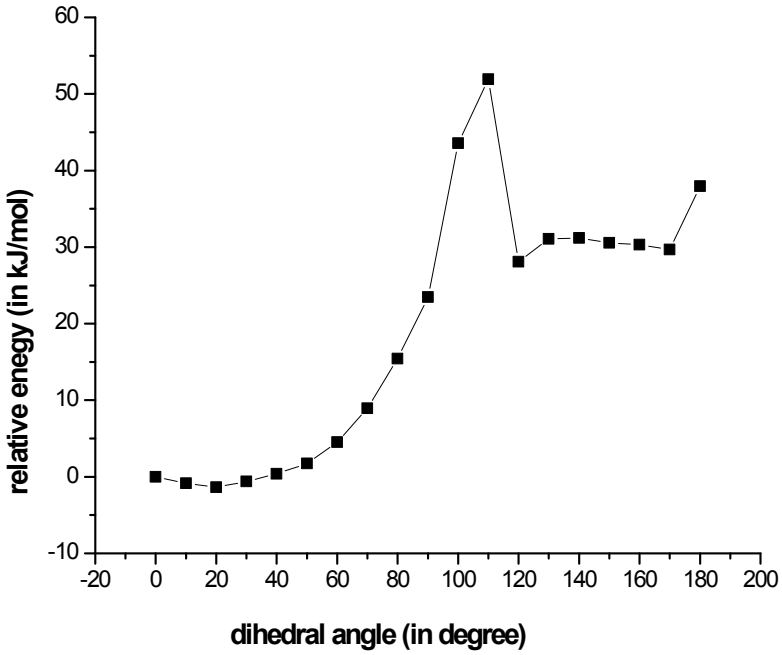

Figure S9. B3LYP computed of relaxed potential-energy scan for dihedral angle rotation from *cis* to *trans* isomer.

When the *trans*-isomer is generating through relaxed scan from the *cis*-isomer where the benzoic acid dihedral angle is rotate in step wise fashion and its maximum estimate is computed to be 51.9 kJ/mol barrier, indicating the likely hood of obtaining both the isomers under ambient conditions.

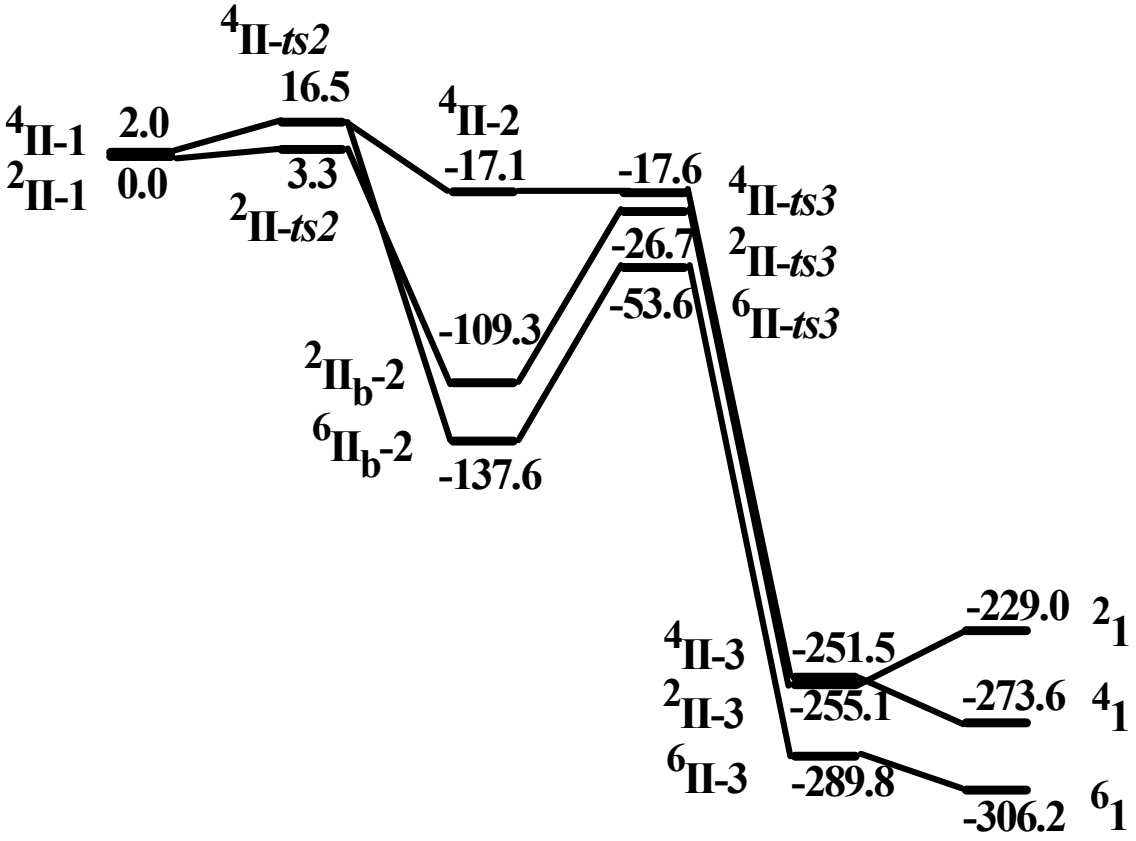

Figure S10. B3LYP computed potential energy surface (ΔG in kJ/mol) for the electrophilic attack pathway for the *ortho*-hydroxylation reaction.

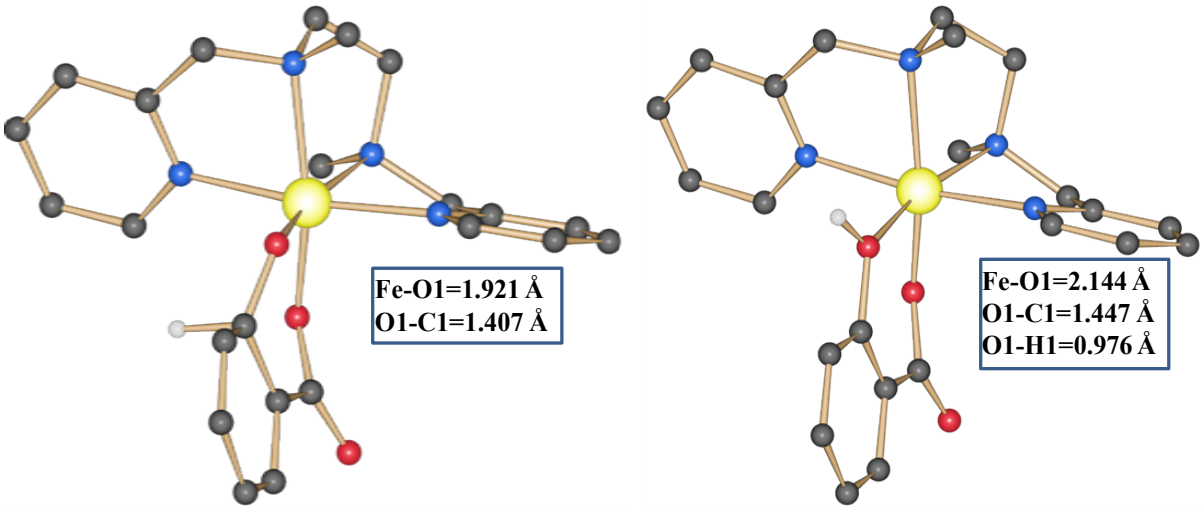

(a) (b)

Figure S11. B3LYP-D optimized structure of the ground state of a) ^{6}II-**2** and b) ^{6}II-**3**.

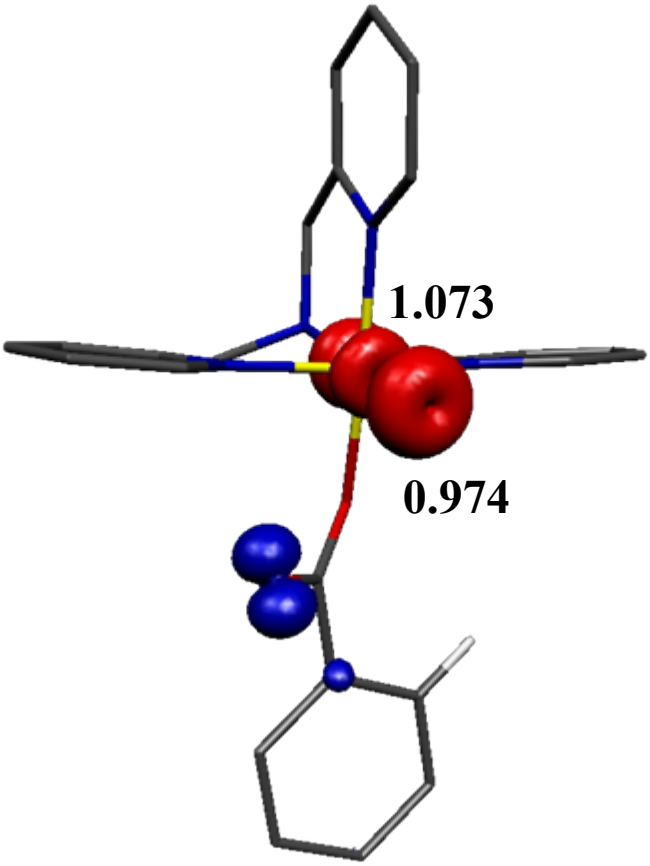

Figure S12. B3LYP-D Computed spin density plot of ^{2}II-**1**(**2**) species.

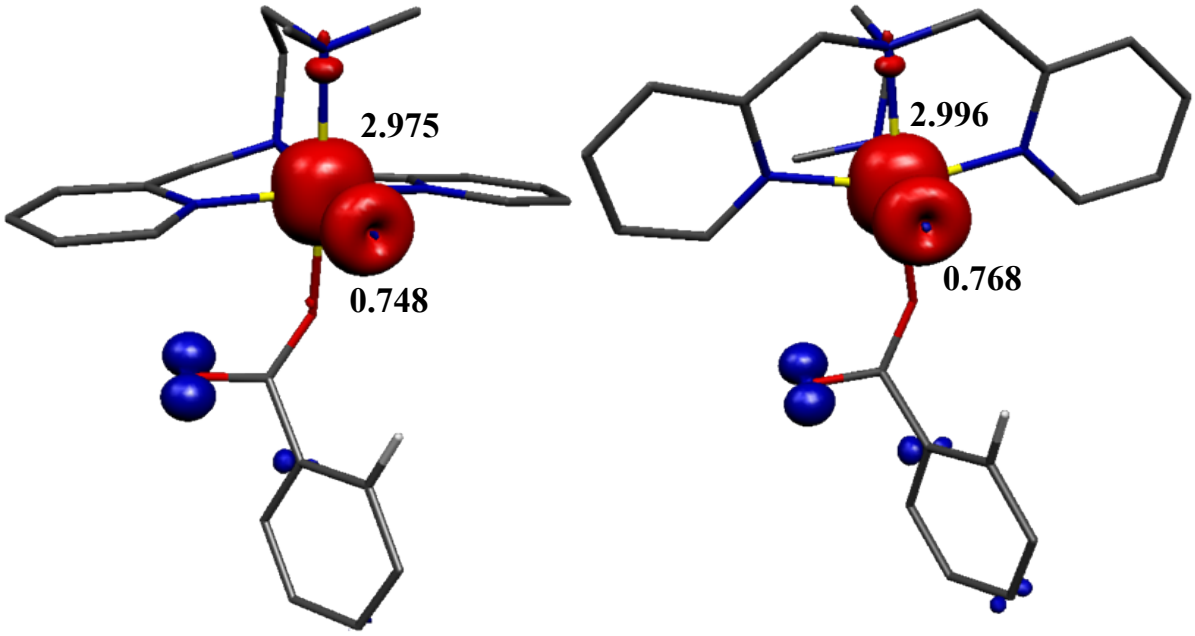

(a) (b)

Figure S13. B3LYP-D computed spin density plots of (a) ^{4}II-**1B** and (b) ^{4}II-**1C**.

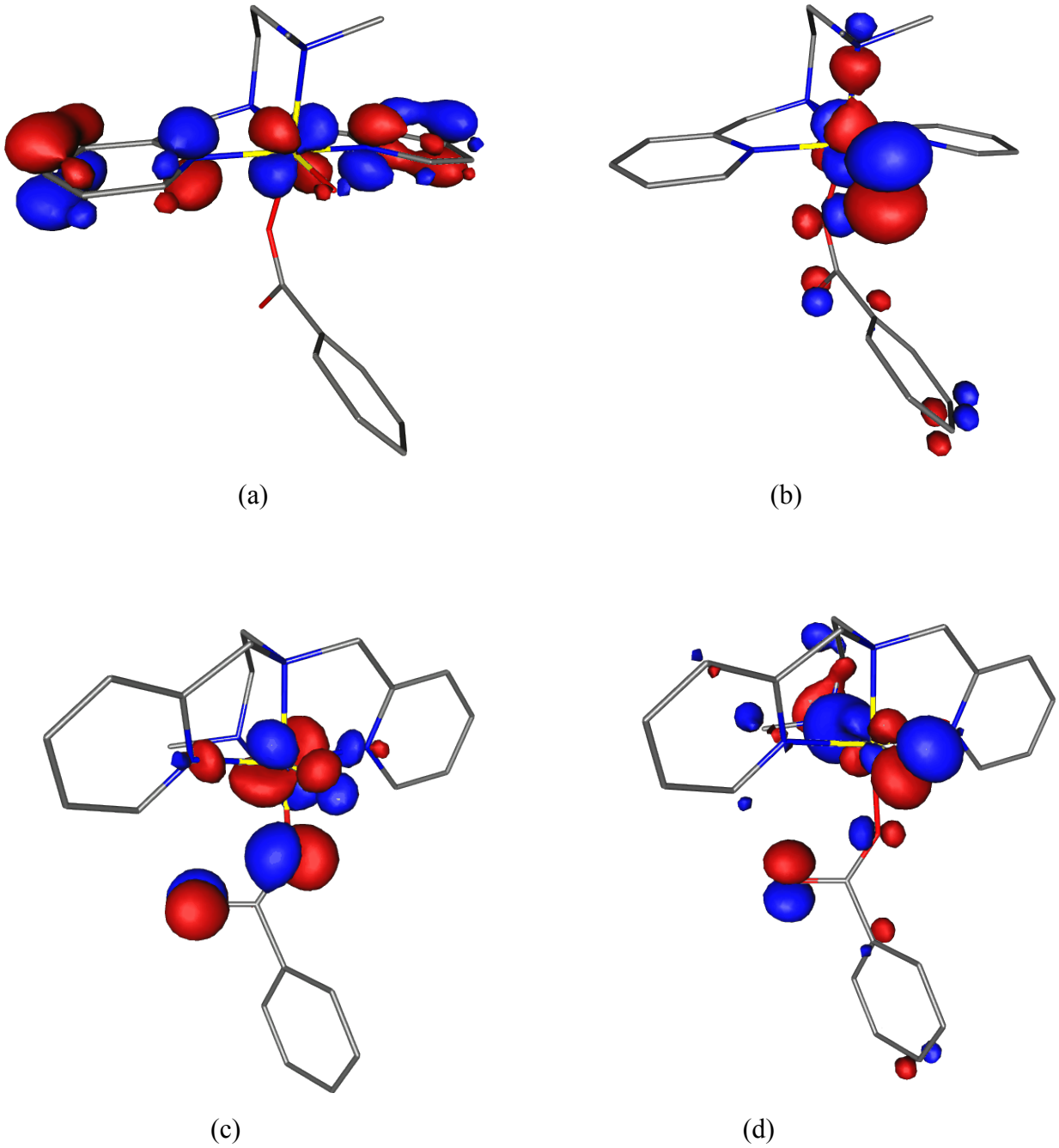

Figure S14. Computed orbitals of a) Fe(d_{xy})^2 and b) Fe(d_{yz}) of II-**1B**); c) Fe(d_{xy})^2 and d) Fe(d_{yz}) of II-**1C**

Table S4. B3LYP-D computed Mulliken spin densities for Fe^{V}=O isomers.

	Fe	O
^{4} II(1)-**1A**	2.985	0.757
^{2} II(1)-**1A**	1.103	0.970
^{4} II(1)-**1B**	2.975	0.748
^{2} II(1)-**1B**	1.131	0.933
^{4} II(1)-**1C**	2.996	0.768
^{2} II(1)-**1C**	1.062	1.019
^{4}II(2)-**1**^{2}	2.985	0.757
^{2}II(2)-**1**^{2}	1.103	0.970

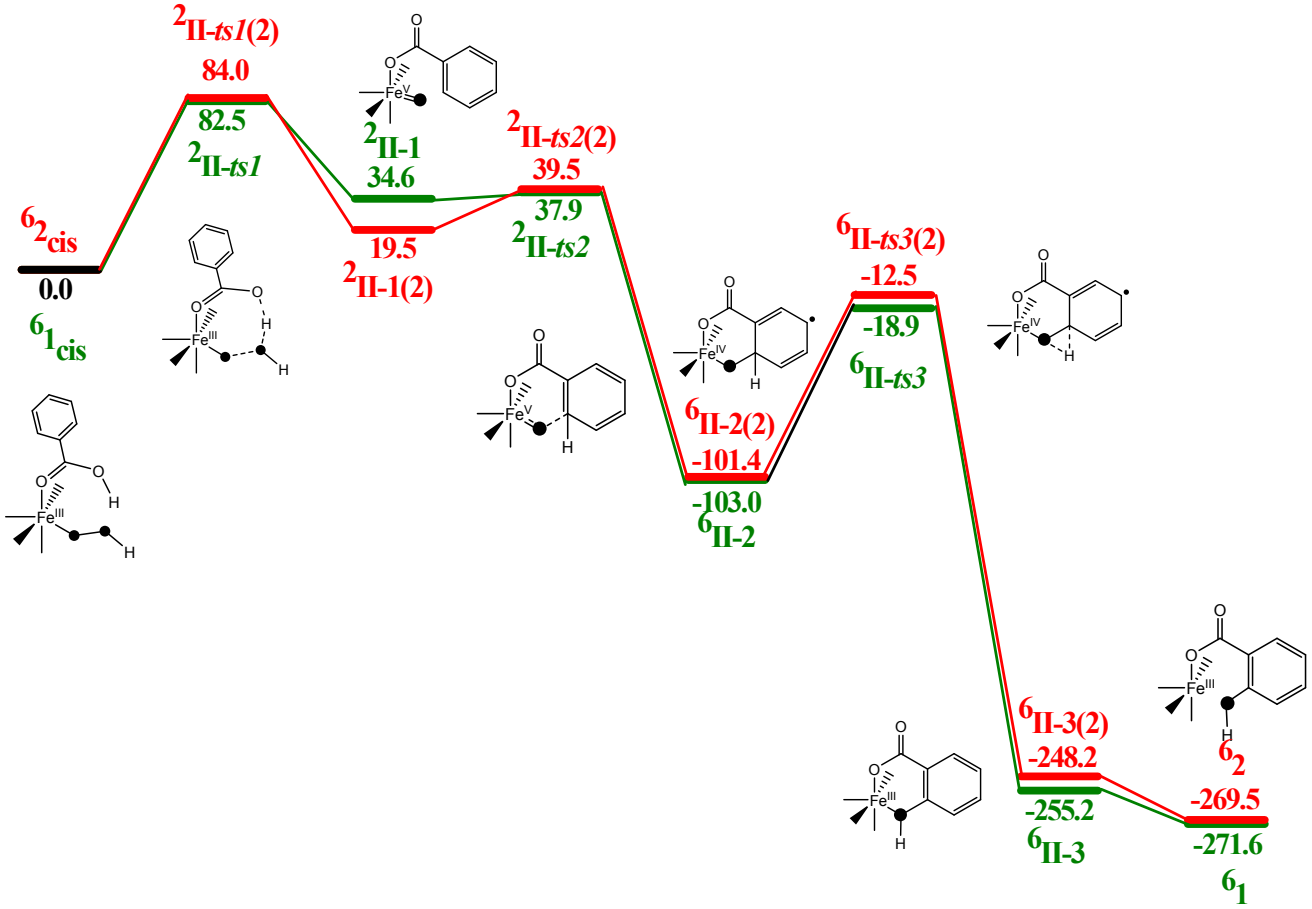

Figure S15. B3LYP computed potential energy surface (ΔG in kJ/mol) (green for BPMEN and red for TPA[2]). All energies are in kJ/mol.

Full reference for reference number 82 which is quoted in the main article

M. J. Frisch, G. W. Trucks, H. B. Schlegel, G. E. Scuseria, M. A. Robb, J. R. Cheeseman, G. Scalmani, V. Barone, B. Mennucci, G. A. Petersson, H. Nakatsuji, M. Caricato, X. Li, H. P. Hratchian, A. F. Izmaylov, J. Bloino, G. Zheng, J. L. Sonnenberg, M. Hada, M. Ehara, K. Toyota, R. Fukuda, J. Hasegawa, M. Ishida, T. Nakajima, Y. Honda, O. Kitao, H. Nakai, T. Vreven, J. A. Montgomery Jr., J. E. Peralta, F. Ogliaro, M. Bearpark, J. J. Heyd, E. Brothers, K. N. Kudin, V. N. Staroverov, R. Kobayashi, J. Normand, K. Raghavachari, A. Rendell, J. C. Burant, S. S. Iyengar, J. Tomasi, M. Cossi, N. Rega, J. M. Millam, M. Klene, J. E. Knox, J. B. Cross, V. Bakken, C. Adamo, J. Jaramillo, R. Gomperts, R. E. Stratmann, O. Yazyev, A. J. Austin, R. Cammi, C. Pomelli, J. W. Ochterski, R. L. Martin, K. Morokuma, V. G. Zakrzewski, G. A. Voth, P. Salvador, J. J. Dannenberg, S. Dapprich, A. D. Daniels, Ö. Farkas, J. B. Foresman, J. V. Ortiz, J. Cioslowski and D. J. Fox, GAUSSIAN 09 (Revision A.1), Gaussian, Inc., Wallingford, CT, 2009.

References

1. F. T. de Oliveira, A. Chanda, D. Banerjee, X. Shan, S. Mondal, L. Que. Jr., E. L. Bominaar, E. Munck and T. J. Collins, Science 2007, **315**, 835-838.
2. A. Ansari, A. Kaushik and G. Rajaraman, *J. Am. Chem. Soc*. 2013, **135**, 4235-4249.